

Dalton Transactions

Accepted Manuscript



This is an *Accepted Manuscript*, which has been through the Royal Society of Chemistry peer review process and has been accepted for publication.

Accepted Manuscripts are published online shortly after acceptance, before technical editing, formatting and proof reading. Using this free service, authors can make their results available to the community, in citable form, before we publish the edited article. We will replace this *Accepted Manuscript* with the edited and formatted *Advance Article* as soon as it is available.

You can find more information about *Accepted Manuscripts* in the [Information for Authors](#).

Please note that technical editing may introduce minor changes to the text and/or graphics, which may alter content. The journal's standard [Terms & Conditions](#) and the [Ethical guidelines](#) still apply. In no event shall the Royal Society of Chemistry be held responsible for any errors or omissions in this *Accepted Manuscript* or any consequences arising from the use of any information it contains.

Structural diversity, spectral and thermal properties of the first alkaline earth metal tetracyanidoborates: $[\text{Mg}(\text{H}_2\text{O})_6][\text{B}(\text{CN})_4]_2$, $[\text{Mg}(\text{H}_2\text{O})_2][\text{B}(\text{CN})_4]_2$, $[\text{Mg}(\text{DMF})_6][\text{B}(\text{CN})_4]_2$, $[\text{Ca}(\text{H}_2\text{O})_3][\text{B}(\text{CN})_4]_2$, and $[\text{Ca}(\text{H}_2\text{O})_2(\text{CH}_3\text{CN})][\text{B}(\text{CN})_4]_2$

Christian Nitschke^a, Martin Köckerling^{*a}, Eduard Bernhardt^{*b}, Torsten Küppers^b and Helge Willner^b

Received (in XXX, XXX) Xth XXXXXXXXX 2013, Accepted Xth XXXXXXXXX 2014

DOI: 10.1039/b000000x

The first members of tetracyanidoborate salts with alkaline earth cations, $[\text{Mg}(\text{H}_2\text{O})_6][\text{B}(\text{CN})_4]_2$ (**1**), $[\text{Mg}(\text{H}_2\text{O})_2][\text{B}(\text{CN})_4]_2$ (**2**), $[\text{Mg}(\text{DMF})_6][\text{B}(\text{CN})_4]_2$ (**3**), $[\text{Ca}(\text{H}_2\text{O})_3][\text{B}(\text{CN})_4]_2$ (**4**), and $[\text{Ca}(\text{H}_2\text{O})_2(\text{CH}_3\text{CN})][\text{B}(\text{CN})_4]_2$ (**5**) were synthesized. Their structures, obtained by single crystal X-ray diffraction, IR- and Raman spectra, as well as thermal properties are determined. Whereas **1** and **3** consist of isolated ions, the other three compounds comprise coordination polymers. IR and Raman spectra give information about the coordination modes of the respective tetracyanidoborate anions. Calorimetric measurements show that the coordinated solvent molecules can be removed at elevated temperatures and anhydrous/solvent free compounds form. The anhydrous compounds are thermally very stable. They do not start to decompose below 500 °C. No melting is observed below decomposition.

Introduction

Over less than the past decade salts with the tetracyanidoborate anion, $[\text{B}(\text{CN})_4]^-$, have emerged as new class of compounds with very interesting structural, chemical, and materials properties. Most of the so far structurally established tetracyanidoborates crystallize in fascinating three-dimensional structures,¹⁻³ or have enabled the formation of unprecedented structural units due to the fact that this anion is relatively large and weakly coordinating.⁴ Tetracyanidoborates have served as starting materials for new weakly coordinating anions like $[\text{B}(\text{CF}_3)_4]^-$ or $[\text{B}(\text{CNB}(\text{C}_6\text{F}_5)_3)_4]^-$ containing salts and for other new materials.⁵⁻⁸ Compounds with weakly coordinating anions (WCA's) are attracting a lot of scientific as well as industrial interest because of various reasons, including their stability against redox agents as well as against acids and bases and their ability to stabilize strong electrophilic cations.⁹ Depending on the type of cation, some WCA's including the tetracyanidoborates are very useful ionic liquids with high thermal stability, large electrochemical windows and low viscosities. They are useful, for example, in solar cells¹⁰ and found application as components of membranes, used in selective separation procedures.¹¹ Others are potential precursors for novel electrolytes or light element ceramics.⁵

When a convenient method using a high temperature solid-state chemical reaction for the synthesis of $\text{K}[\text{B}(\text{CN})_4]$ was introduced in 2003, a systematic study of tetracyanidoborates with different cations has been started.¹² A further and very useful, general route to new tetracyanidoborates was opened, when the preparation and

structure of the stable tetracyanidoborate acid was published in 2007.²⁰ So far, the tetracyanidoborates $M^l[\text{B}(\text{CN})_4]$ with the monovalent cations $M^l = \text{Li}^+ - \text{Cs}^+$, Hg^+ , Cu^+ , Tl^+ , $[\text{NH}_4]^+$, $[\text{PPh}_4]^+$ and Ag^+ , have been characterised.^{1,2,13,14b} Tetracyanidoborate salts with divalent cations are known with the transition metal cations Cu^{2+} , Zn^{2+} , Cd^{2+} , Hg^{2+} , Mn^{2+} , Ni^{2+} , Fe^{2+} , and Co^{2+} .^{2,14a,15,16,17} Also, the first tetracyanidoborate with a triply charged cation, $[\text{Fe}(\text{H}_2\text{O})_6][\text{B}(\text{CN})_4]_3$, was synthesized and characterized.¹⁷ In addition, some structures with sterical demanding organic cations and some with crown ether ligands attached to the cations have been published.^{18,19}

In this paper we present the syntheses, structures, and spectroscopic, as well as thermal properties of the new materials $[\text{Mg}(\text{H}_2\text{O})_6][\text{B}(\text{CN})_4]_2$ (**1**), $[\text{Mg}(\text{H}_2\text{O})_2][\text{B}(\text{CN})_4]_2$ (**2**), $[\text{Mg}(\text{DMF})_6][\text{B}(\text{CN})_4]_2$ (**3**), $[\text{Ca}(\text{H}_2\text{O})_3][\text{B}(\text{CN})_4]_2$ (**4**), and $[\text{Ca}(\text{H}_2\text{O})_2(\text{CH}_3\text{CN})][\text{B}(\text{CN})_4]_2$ (**5**), which are the first alkaline earth tetracyanidoborates.

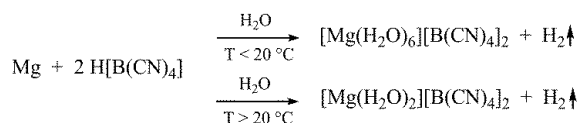
Results and Discussion

Syntheses

Extensive investigations of the chemical reactivity, physical properties, and structures of new tetracyanidoborates have emerged quickly, when the efficient synthetic procedure of $\text{K}[\text{B}(\text{CN})_4]$ as starting material for new compounds was developed in 2003.¹² This procedure allows to prepare molar amounts of tetracyanidoborate salts through a high temperature process in ~60% yield. Starting from $\text{K}[\text{B}(\text{CN})_4]$ a variety of new tetracyanidoborate salts is accessible by ion exchange or metathesis reactions.¹ Another way to new tetracyanidoborates uses the acid $\text{H}[\text{B}(\text{CN})_4]$, which can be easily obtained by an ion exchange process.²⁰

$[\text{Mg}(\text{H}_2\text{O})_6][\text{B}(\text{CN})_4]_2$ (**1**) and $[\text{Mg}(\text{H}_2\text{O})_2][\text{B}(\text{CN})_4]_2$ (**2**): For the magnesium tetracyanidoborate hydrates **1** and **2** the reaction of elemental magnesium with $\text{H}[\text{B}(\text{CN})_4]$ was chosen because of the high reducing power of Mg and the high acidity of $\text{H}[\text{B}(\text{CN})_4]$. The reaction is sketched in Scheme 1:

- [a] Institut für Chemie
Anorganische Chemie / Festkörperchemie
Universität Rostock
Albert-Einstein-Str 3a
D-18059 Rostock/Germany
Tel.: +49 (0)381 498 6390
Fax: +49 (0)381 498 6382
E-mail: Martin.Koeckerling@uni-rostock.de
- [b] FB C – Anorganische Chemie
Bergische Universität Wuppertal
Gaußstraße 20
D-42119 Wuppertal/Germany
Tel.: +49(0)202 439 2502
Fax: +49(0)202 439 3053
E-Mail: edbern@uni-wuppertal.de



Scheme 1. Reactions, from which the new magnesium tetracyanidoborates **1** and **2** are obtained.

Single crystals of $[\text{Mg}(\text{H}_2\text{O})_6][\text{B}(\text{CN})_4]_2$ precipitate from aqueous solution at temperatures below 20°C while at higher temperatures $[\text{Mg}(\text{H}_2\text{O})_2][\text{B}(\text{CN})_4]_2$ forms.

$[\text{Mg}(\text{DMF})_6][\text{B}(\text{CN})_4]_2$ (**3**): The DMF adduct of the magnesium salt can be synthesized by dissolving solvent free $\text{Mg}[\text{B}(\text{CN})_4]_2$ in dry DMF and subsequent crystallisation. Anhydrous $\text{Mg}[\text{B}(\text{CN})_4]_2$ is obtained by heating of **1** or **2** at 160°C for 5 hrs under ambient pressure.

$[\text{Ca}(\text{H}_2\text{O})_3][\text{B}(\text{CN})_4]_2$ (**4**) and $[\text{Ca}(\text{H}_2\text{O})_2(\text{CH}_3\text{CN})][\text{B}(\text{CN})_4]_2$ (**5**): For the synthesis of the calcium salts **4** and **5** the route via tri-*n*-

propylammonium tetracyanidoborate was chosen, from which the calcium salt $[\text{Ca}(\text{H}_2\text{O})_3][\text{B}(\text{CN})_4]_2$ is easily obtained by addition of $\text{Ca}(\text{OH})_2$. This procedure has been shown to be efficient for those metals, which form soluble strong bases.¹ Compound **5** is synthesized by dissolving **4** in acetonitrile and subsequent crystallisation.

Structures

Crystals of the new tetracyanidoborates **1-5**, which are suitable for single-crystal X-ray determinations, are easily available from solutions of the respective salts. Salt **1** crystallizes at temperatures below 20°C , **2** above 20°C by slow evaporation of the solvent (water). Colourless single crystals of **3** were obtained after slow evaporation of the DMF solvent off a saturated solution in a drybox or using Schlenk equipment. Similarly, crystals of **4** are obtained from aqueous solutions, of **5** from a solution of **4** in acetonitrile. Crystallographic data of the five title compounds are collected in Table 1.

Table 1. Crystallographic data of the tetracyanidoborates $[\text{Mg}(\text{H}_2\text{O})_6][\text{B}(\text{CN})_4]_2$ (**1**), $[\text{Mg}(\text{H}_2\text{O})_2][\text{B}(\text{CN})_4]_2$ (**2**), $[\text{Mg}(\text{DMF})_6][\text{B}(\text{CN})_4]_2$ (**3**), $[\text{Ca}(\text{H}_2\text{O})_3][\text{B}(\text{CN})_4]_2$ (**4**), and $[\text{Ca}(\text{H}_2\text{O})_2(\text{CH}_3\text{CN})][\text{B}(\text{CN})_4]_2$ (**5**).

	1	2	3	4	5
formula	$\text{C}_8\text{H}_{12}\text{B}_2\text{MgN}_8\text{O}_6$	$\text{C}_8\text{H}_4\text{B}_2\text{MgN}_8\text{O}_2$	$\text{C}_{26}\text{H}_{42}\text{B}_2\text{MgN}_{14}\text{O}_6$	$\text{C}_8\text{H}_6\text{B}_2\text{CaN}_8\text{O}_3$	$\text{C}_{10}\text{H}_{15}\text{B}_2\text{CaN}_9\text{O}_2$
fw (g/mol)	362.19	290.01	692.63	323.91	346.95
T (K)	150(2)	295(2)	173(2)	173(2)	213(2)
cryst. syst.	triclinic	tetragonal	triclinic	triclinic	monoclinic
space group	$P\bar{1}$ (no. 2)	$I\bar{4}2d$ (no. 122)	$P\bar{1}$ (no. 2)	$P\bar{1}$ (no. 2)	$P2_1/c$ (14)
Z	2	4	1	2	4
a (Å)	9.0078(8)	12.3940(4)	8.6187(4)	9.5347(2)	12.2203(2)
b (Å)	9.7507(7)	12.3940(4)	11.1119(5)	10.2205(2)	12.6637(2)
c (Å)	11.589(1)	9.2041(3)	12.2149(5)	10.4874(2)	13.5191(2)
α (°)	82.034(7)	90	66.096(2)	68.283(1)	90
β (°)	68.642(9)	90	75.570(2)	89.223(1)	116.538(1)
γ (°)	72.303(7)	90	76.422(2)	63.152(1)	90
V (Å ³)	902.7(7)	1413.85(8)	1023.9(1)	832.45(3)	1871.71(5)
$\rho_{\text{calc.}}$ (g·cm ⁻³)	1.333	1.363	1.123	1.292	1.231
μ (mm ⁻¹)	0.14	0.14	0.10	0.397	0.356
λ (Å)	0.71073	0.71073	0.71073	0.71073	0.71073
no. parameters	274	52	224	223	234
GOF on F^2	1.044	1.055	1.072	1.067	1.035
R indices	$R1 = 0.0308$,	$R1 = 0.0253$,	$R1 = 0.0450$,	$R1 = 0.0279$	$R1 = 0.0346$,
$[I > 2\sigma(I)]^{\text{a,b,c}}$	$wR2 = 0.0718$	$wR2 = 0.0621$	$wR2 = 0.1443$	$wR2 = 0.0785$	$wR2 = 0.0867$
weighting					
A/B ^c	0.0295/0.2009	0.0375/0.0416	0.0836/0.0407	0.0403/0.0922	0.0490/0.1313

$$^{\text{a}} R1 = \frac{\sum |F_o| - |F_c|}{\sum |F_c|}; \quad ^{\text{b}} wR2 = \sqrt{\frac{\sum \{w(F_o^2 - F_c^2)^2\}}{\sum \{w(F_o^2)^2\}}};$$

$$^{\text{c}} w = 1/[(\sigma^2(F_o^2) + (A \cdot P)^2 + B \cdot P)]; \quad P = (F_o^2 + 2 F_c^2)/3$$

compounds contain Mg^{2+} cations, which are octahedrally coordinated. In **1** the Mg^{2+} cations are bonded to the O atoms of six

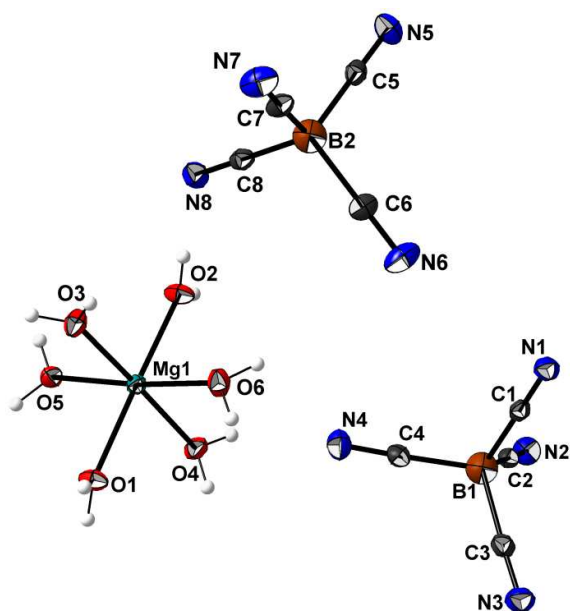


Fig. 1. View of the atom arrangement of the structure forming ions with the octahedral coordination environment of the Mg1 ion in crystals of $[\text{Mg}(\text{H}_2\text{O})_6][\text{B}(\text{CN})_4]_2$ with atom labelling scheme. Displacement ellipsoids are drawn at the 50% probability level.

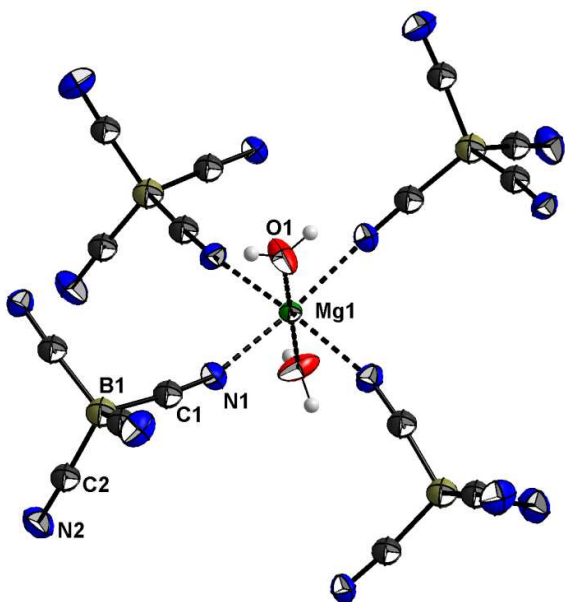


Fig. 2. View of the octahedral coordination environment of the Mg^{2+} ion in crystals of $[\text{Mg}(\text{H}_2\text{O})_2][\text{B}(\text{CN})_4]_2$ with atom labelling scheme. Displacement ellipsoids are drawn at the 50% probability level.

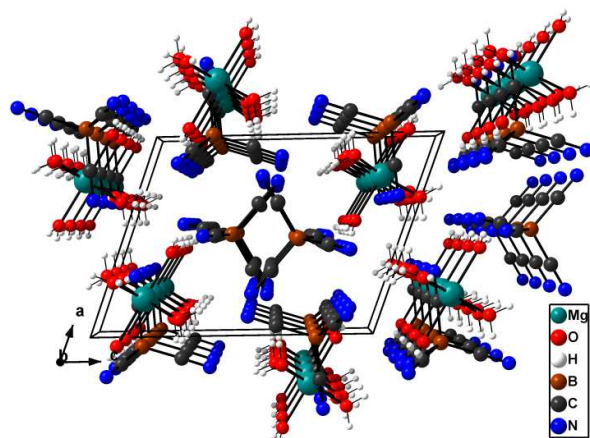
$[\text{Mg}(\text{H}_2\text{O})_6][\text{B}(\text{CN})_4]_2$ (**1**) and $[\text{Mg}(\text{H}_2\text{O})_2][\text{B}(\text{CN})_4]_2$ (**2**)

Crystals of **1** contain isolated $[\text{Mg}(\text{H}_2\text{O})_6]^{2+}$ cations and $[\text{B}(\text{CN})_4]^-$ anions with triclinic symmetry of space group $P\bar{1}$. Compound **2** crystallizes isostructurally with $[\text{M}^{\text{II}}(\text{H}_2\text{O})_2][\text{B}(\text{CN})_4]_2$ ($\text{M}^{\text{II}} = \text{Co}, \text{Fe}, \text{Zn}, \text{Mn}$) in the tetragonal space group $I42d$. Both

Tab. 2. Selected atom distances (Å) within **1** – **5**.

	1	2	3	4	5
cation:					
M^{II} –O	2.0373(9)-2.091(1)	2.0374(8)	2.0483(6)-2.0689(7)	2.3800(4)-2.5135(4)	2.3680(7)-2.4702(6)
average	2.061	2.037	2.059	2.456	2.419
M^{II} –N	–	2.1843(7)	–	2.5375(5)-2.5615(5)	2.5650(8)-2.5983(8) 2.5271(9) (Ca–N _{acetonitril})
average	–	2.184	–	2.552	2.587
anion:					
B–C	1.587(2)-1.599(2)	1.592(1)-1.599(1)	1.588(2)-1.594(2)	1.5848(7)-1.5920(7)	1.587(2)-1.594(1)
average	1.594	1.595	1.591	1.589	1.590
C–N	1.139(2)-1.140(2)	1.135(1)-1.139(1)	1.138(2)-1.143(2)	1.1479(7)-1.1500(8)	1.140(1)-1.143(1) 1.135(1) (acetonitril)
average	1.139	1.137	1.140	1.149	1.140

water molecules, whereas in **2** they are bonded to two oxygen atoms of water molecules, *trans* to each other, and four nitrogen atoms of four different tetracyanidoborate anions. Views of the octahedral coordination environments of the Mg^{2+} ion and the structures of the tetracyanidoborate anions in crystals of both compounds with the atom labelling scheme are given in Figures 1 and 2. Bond lengths for **1** and **2** (as well as for the other title compounds) are given in Table 2, bond angles in Table 3. In **1**, the coordination environment around the Mg^{2+} ion deviates marginally from ideal octahedral, as visible from the angles in Table 1. Similar, the environment around the B atom of the anion deviates from ideal tetrahedral. The packing of the isolated ions in **1** is shown in Figure 3.

**Fig. 3.** View of structure of $[Mg(H_2O)_6][B(CN)_4]_2$ approximately along the *b* direction showing the arrangement of complex ions.

With shorter Mg–O distances (2.0374(8) Å) than the Mg–N distances (2.1843(7) Å) in **2** the coordination sphere of the metal ion can be described as a distorted compressed octahedron with O–M–N angles deviating from 90° by ±4.99° (see Table 3). Two of the cyanido groups of each $[B(CN)_4]^-$ unit coordinate to two neighbouring Mg^{2+} ions. The result is a three-dimensional network structure of tetracyanidoborate anions bridging the magnesium cations, expressed by $[Mg^{II}(H_2O)_2\{\kappa^2N[B(CN)_4]\}_2]_n$, (Figure 4). This arrangement reminds of the cubic CaF_2 structure, wherein the $Mg(H_2O)_2N_4$ units replace the calcium ions and the BC_4 units

occupy all tetrahedral holes. The cationic units do not form a face-centered arrangement, because every second unit is being shifted away from the face centers along the *c* axis. Therefore, the symmetry is reduced to body-centered tetragonal. The M–N and M–O bond distances of the five tetracyanidoborates $[M^{II}(H_2O)_2][B(CN)_4]_2$ ($M^{II} = Mg^{2+}, Co^{2+}, Fe^{2+}, Zn^{2+}, Mn^{2+}$) are compared in Table 4, which lists also the revised Shannon effective ionic radii for the M^{II} cations with coordination number 6.²¹ The M–O distances increase in the order $M^{II} = Mg, Zn, Co, Fe$, to Mn as do in the same sequence the Shannon radii. This sequence is followed also roughly by the M–N distances taking into account that the single-crystal X-ray diffraction data have been measured at different temperatures. Deviations are likely to originate from differences in specific bonding situations. This structural comparison assumes the M^{II} ions to be in the high spin configurations. At least for the $M = Fe$ case at lower temperature transition into the low-spin state might occur, as observed for other Fe^{II} compounds with a N_4O_2 coordination sphere.²²

Within the $[B(CN)_4]^-$ anion in **2** two of the CN groups are bonded to the magnesium cation, whereas the other two are non-coordinating. Thereby, the anion is distorted from ideal tetrahedral with C–B–C angles ranging from 105.46(2)° to 111.59(2)°. This is also visible in the vibrational spectra where two different C–N absorption frequencies are observed. The C–N and B–C bond distances in **1** are similar to those found in other tetracyanidoborates with divalent or singly charged cations.^{1,2,14-19}

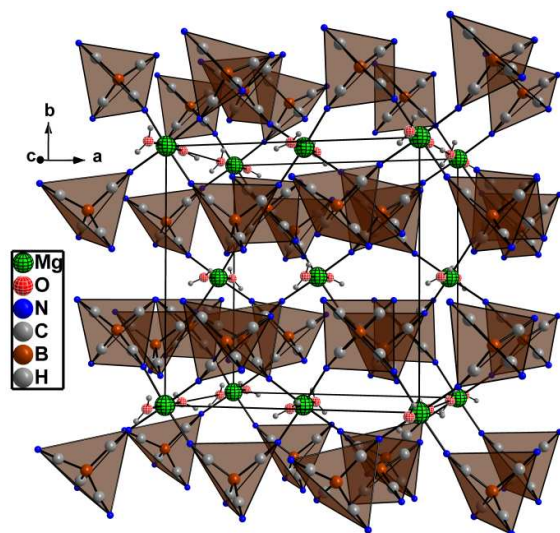


Fig. 4. Representation of the structure of $[\text{Mg}(\text{H}_2\text{O})_2][\text{B}(\text{CN})_4]_2$ approximately along the c direction showing the layered arrangement of ions. The tetrahedral tetracyanidoborate anions are shown as polyhedra.

$[\text{Mg}(\text{DMF})_6][\text{B}(\text{CN})_4]_2$ (**3**) crystallizes isostructurally with $[\text{Fe}(\text{DMF})_6][\text{B}(\text{CN})_4]_2$ and $[\text{Zn}(\text{DMF})_6][\text{B}(\text{CN})_4]_2$ in the triclinic space group $P\bar{1}$ (no. 2).^{17,23} The structure contains isolated cations, composed of magnesium(II) ions, which are octahedrally surrounded by 6 molecules of dimethylformamide and isolated tetracyanidoborate anions as counterions. A view of the coordination environment of the Mg^{2+} ions as thermal ellipsoid plot with the atom-labelling scheme is given in Figure 5.

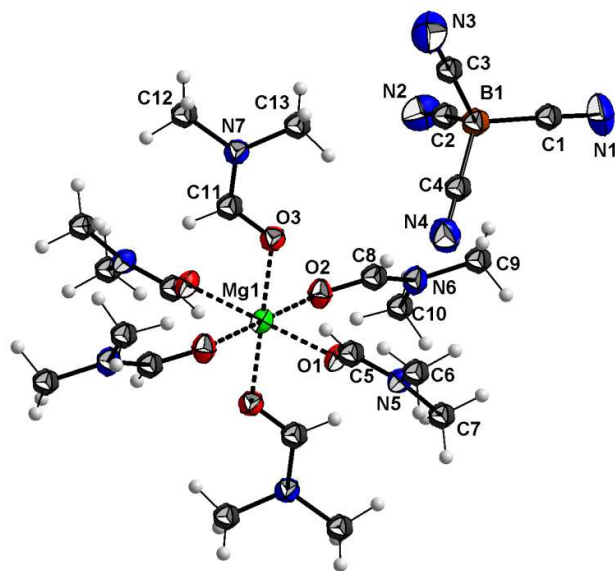


Fig. 5. View of the octahedral coordination environment of the Mg1 ion in crystals of $[\text{Mg}(\text{DMF})_6][\text{B}(\text{CN})_4]$ with atom labelling scheme. Displacement ellipsoids are drawn at the 50% probability level.

The metal ion is located on a site with inversion symmetry. The Mg–O distances vary between 2.0483(6) and 2.0689(7) Å (average 2.0592 Å) with O–Mg–O angles ranging from 88.32(4)° to 91.67(4)°. These distances and angles compare very well with those of other compounds containing $[\text{Mg}(\text{DMF})_6]^{2+}$ octahedra,

like, for example, $[\text{Mg}(\text{DMF})_6][\text{MgCl}_4]$ (average Mg–O distances: 2.054 and 2.076 Å for the two independent cations).²⁴ Direct coordination between the cyanido nitrogen atoms and the magnesium(II) ions or hydrogen bonding is not observed in **3**, but, nevertheless, the tetracyanidoborate anion is slightly distorted in this compound ($\text{C–B–C}_{\text{range}}$: 107.85°–110.72°, see Table 3). The reason for the distortion could be van-der-Waals interactions of

Tab. 3. Selected bond angles (°) in **1** – **5**.

1		2	
atoms	angle	Atoms	angle
cation:			
O1–Mg1–O1 ^{a, #1}	84.75(4)-94.36(4)	O1–Mg1–O1 ^{a, #1}	180.0
	172.84(4)-177.61(4)	O1–Mg1–N1	85.01(2)
		N1–Mg1–N1 ^{a, #1}	90.434(4)
anion:			
C–B–C	107.5(1)-111.3(1)	C–B–C	105.46(9)-111.58(9)
N–C–B	176.4(1)-179.4(1)	N–C–B	174.53(8)-177.45(9)
3		4	
Atoms	Angle	atoms	angle
cation:			
O–Mg1–O	87.98(3)-92.02(3)	O–Ca1–O ^b	71.63(1)-81.75(2)
		O–Ca1–O ^c	110.08(2)-143.79(2)
		O–Ca1–N ^b	70.11(2)-88.48(2)
		O–Ca1–N ^c	116.93(2)-145.38(2)
		N–Ca1–N ^b	70.51(2)-78.10(2)
		N–Ca1–N ^c	110.30(2)-137.92(2)
anion:			
C–B–C	107.79(9)-110.7(1)	C–B–C	107.04(4)-112.94(5)
N–C–B	177.9(1)-178.9(1)	N–C–B	174.37(7)-178.96(6)
5			
atoms	Angle		
cation:			
O1–Ca1–O2	75.57(3)		
O–Ca1–N ^b	71.53(2)-83.26(3)		
O–Ca1–N ^c	117.27(3)-149.81(3)		
N–Ca1–N ^b	69.98(3)-77.67(3)		
N–Ca1–N ^c	90.12(3)-148.33(3)		
anion:			
C–B–C	108.26(8)-111.03(8)		
N–C–B	175.78(9)-179.32(9)		

^a Symmetry operations used to generate equivalent atoms: #1: $y+\frac{1}{2}, \frac{1}{2}-x, \frac{1}{2}-z$;

^b acute angles; ^c obtuse angles

Tab. 4. Comparison of *M*–N and *M*–O bond distances (Å) in $[M^{\text{II}}(\text{H}_2\text{O})_2][\text{B}(\text{CN})_4]_2$ (M^{II} = Co, Fe, Zn, Mn, and Mg).

bond	<i>M</i> = Co	<i>M</i> = Fe	<i>M</i> = Zn	<i>M</i> = Mn	<i>M</i> = Mg
<i>M</i> –N	2.124(2)	2.168(2)	2.145(1)	2.237(1)	2.1843(7)
<i>M</i> –O	2.059(2)	2.072(2)	2.055(1)	2.137(1)	2.0373(8)
Shannon effective ionic radius for M^{2+} [21]	0.885 ^a	0.920 ^a	0.880 ^a	0.970 ^a	0.860

^a high-spin configuration

different strengths between the cyanido groups and the surrounding DMF molecules. The C–N and B–C bond distances of the anion are in good agreement with those of other tetracyanidoborates with divalent or singly charged cations.^{1,14-19} Figure 6 shows the arrangement of the molecular ions within the unit cell. The large complex cations are lined up in layers along the *c* direction, and in between these layers the smaller anions are located.

$[\text{Ca}(\text{H}_2\text{O})_2][\text{B}(\text{CN})_4]_2$ (**4**) crystallizes also in the triclinic space group $P\bar{1}$ (no. 2). The structure contains Ca^{2+} cations, which are coordinated by four oxygen atoms of water molecules and four

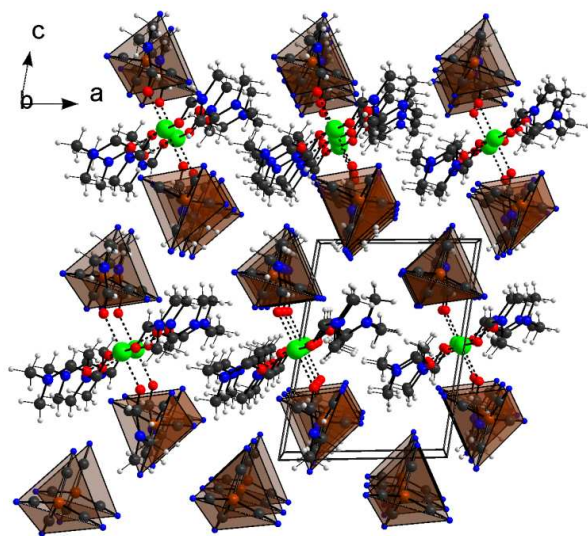


Fig. 6 The three-dimensional structure of $[\text{Mg}(\text{DMF})_6][\text{B}(\text{CN})_4]$ in a view along the b direction showing the arrangement of isolated ions. The anions are shown as polyhedra.

nitrogen atoms of four different tetracyanidoborate anions. A view of the coordination environment of the Ca^{2+} ions is given in Figure 7.

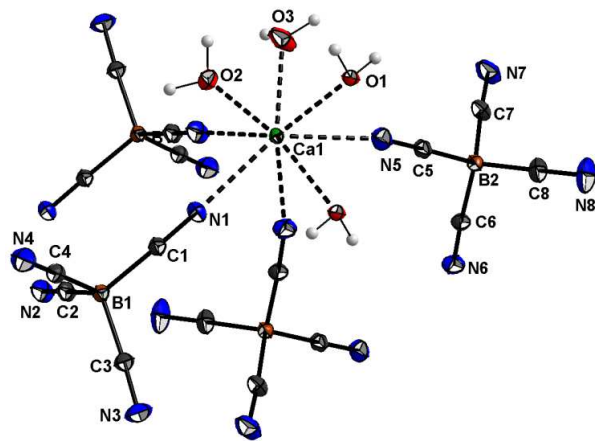


Fig. 7 View of the coordination environment of the Ca^{2+} ion in crystals of $[\text{Ca}(\text{H}_2\text{O})_3][\text{B}(\text{CN})_4]_2$ with atom labelling scheme. Displacement ellipsoids are drawn at the 50% probability level.

The Ca–O distances vary between 2.3800(4) and 2.5135(4) Å and the Ca–N distances between 2.5375(5) and 2.5615(5) Å (Table 2). The coordination environment of the calcium ions can be described as a distorted square antiprism. Similar to the anions in **2** two of the cyanido groups of each $[\text{B}(\text{CN})_4]^-$ unit coordinate two neighbouring Ca^{2+} ions. The result is a three-dimensional network structure of tetracyanidoborate anions bridging the calcium cations, expressed by $[\text{Ca}^{\text{II}}(\text{H}_2\text{O})_2\{\kappa^2\text{N}[\text{B}(\text{CN})_4]\}_2\{\kappa^2\text{O}(\text{H}_2\text{O})\}]_n$ (Figure 8). The differences between the coordination polymer of **2** and **4** originate from the different size of the corresponding cations Mg^{2+} and Ca^{2+} . The effective ionic radii according to Shannon are 0.86 Å for Mg^{2+} and 1.26 Å for Ca^{2+} . Hence, there are two more molecules of water in the coordination sphere of the calcium ion compared to

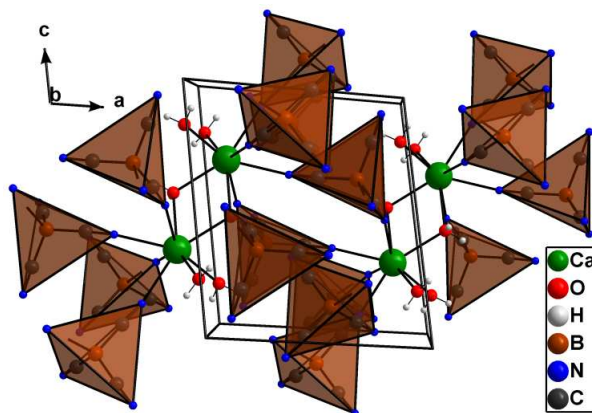


Fig. 8 Crystal structure of $[\text{Ca}(\text{H}_2\text{O})_3][\text{B}(\text{CN})_4]_2$ shown as an arrangement of $[\text{B}(\text{CN})_4]$ tetrahedra separated by the calcium ions, which have additional water molecules coordinated.

the Mg ion. In **4** the O atoms of two of the water molecules (O1 x2) are bridging metal ions and two are non-bridging water molecules (O2 and O3). O1 is located on a site with inversion symmetry. Due to the larger Shannon radii of the Ca^{2+} ion the $M^{\text{II}}\text{--N}$ and $M^{\text{II}}\text{--O}$ distances are longer compared to those in the $[\text{M}^{\text{II}}(\text{H}_2\text{O})_2][\text{B}(\text{CN})_4]_2$ ($M^{\text{II}} = \text{Mg}, \text{Co}, \text{Fe}, \text{Zn}, \text{Mn}$) compounds. As in compound **2** two of the CN groups within the $[\text{B}(\text{CN})_4]^-$ anion are coordinated to the metal ion, whereas two CN groups are non-coordinating. As a consequence a distortion of the tetracyanidoborate anion is observed with C–B–C angles ranging from 107.04° to 112.94° (Table 3). This is also visible in the vibrational spectra where two different C–N absorption frequencies are observed (see below). The C–N and B–C bond distances in **4** are similar to those found in other tetracyanidoborates with divalent or singly charged cations (Tables 2 and 4).^{1,2,14-19}

$[\text{Ca}(\text{H}_2\text{O})_2(\text{CH}_3\text{CN})][\text{B}(\text{CN})_4]_2$ (**5**) crystallizes in the monoclinic space group $\text{P}2_1/\text{c}$ (no. 14). The structure contains Ca^{2+} ions which are coordinated by N atoms of five different tetracyanidoborate anions, two molecules of water and one molecule of acetonitrile. A view of the coordination environment of the Ca^{2+} ion is given in Figure 9.

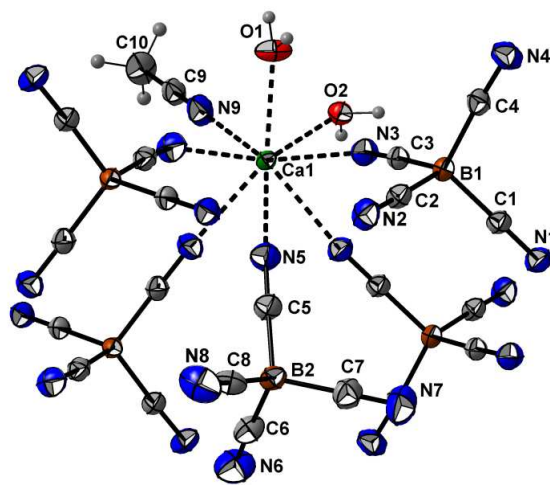


Fig. 9 View of the coordination environment of the Ca^{2+} ion in crystals of $[\text{Ca}(\text{H}_2\text{O})_2(\text{CH}_3\text{CN})][\text{B}(\text{CN})_4]_2$ with atom labelling scheme. Displacement ellipsoids are drawn at the 50% probability level.

The Ca–O distances are 2.3680(7) Å (Ca1–O1) and 2.4702(6) Å (Ca1–O2, see Table 2). The N atom of the coordinated acetonitrile molecule has a shorter distance to the Ca²⁺ ion (2.5271(3) Å) than the N atoms of the tetracyanidoborate anions, with an average value of 2.587 Å. The coordination environment of the Ca²⁺ ion in **5** can also be described as a distorted square antiprism with angles in the square base deviating by a maximum of ~8° from 90°. In contrast to compound **2** and **4** four of the cyanido groups of one tetracyanidoborate anion (B1) coordinate four neighbouring Ca²⁺ ions whereas just one cyanido group of the second symmetry independent tetracyanidoborate anion (B2) coordinates one calcium ion. The three remaining CN groups around B2 are non-coordinating. The result is an interesting three-dimensional structure with layers of interconnected tetracyanidoborate anions and Ca²⁺ cations in the b-c plane expressed by [Ca^{II}(H₂O)₂(CH₃CN){κ⁴N[B(CN)₄]}[B(CN)₄]_n. These layers are in turn connected with each other by hydrogen bonds between the water molecules which are coordinated to the metal ions. With an O1–O2 distance of 2.843 Å the hydrogen bonds in **5** can be considered as strong hydrogen bonds, comparable with the hydrogen bonds in ice, which show O–O distances of 2.6 to 2.8 Å. Figure 10 shows these layers extending in the b-c plane. In-between these layers of tetracyanidoborate anions and cations the acetonitrile and water molecules are located. The [B(CN)₄][−] anions in **5** are also slightly distorted from ideal tetrahedral with C–B–C angles ranging from 108.3° to 111.0°. Again, the reason is the non-symmetric coordination environment around both the [B(CN)₄][−] ions. In the tetracyanidoborate anion around B2 only one CN group is coordinating the metal ion whereas the other three are non-coordinating. The other anion, which is more symmetrically coordinated by four calcium ions, is also distorted. This might be explained by the different interaction strengths of the water molecules in the coordination sphere of the Ca²⁺ ion, which in turn also influences the tetracyanidoborate CN groups. These interactions can also be interpreted as weak hydrogen bonds causing the distortion of the anion. The C–N and B–C bond distances in **5** are similar to those found in other tetracyanidoborates with divalent or singly charged cations (Table 2).^{1,2,14-19}

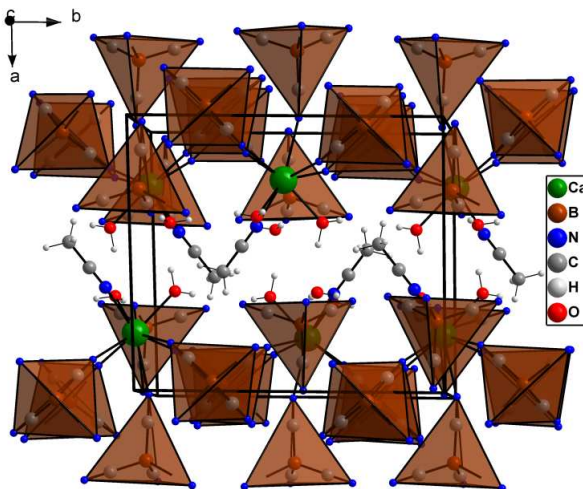


Fig. 10. A view of the structure of [Ca(H₂O)₂(CH₃CN)][B(CN)₄]₂ projected along the *c* axis. The [B(CN)₄][−] anions are shown as polyhedral.

Spectra

From samples of all five title compounds as well as from anhydrous samples of **2** and **4** vibrational spectra have been recorded (Figures 11 and 12). Comparing the IR with the Raman spectra the CN vibrations appear in both spectra almost at the same frequency. A complete analysis of the spectrum of [B(CN)₄][−] is given in ref. 13.

The magnesium salt [Mg(H₂O)₂][B(CN)₄]₂ shows four CN stretching modes at 2234, 2246, 2263, and 2268 (shoulder) cm^{−1} in the IR spectrum. The corresponding Raman spectrum shows also four vibrational bands at 2235, 2248, 2264 (with shoulder) cm^{−1}. According to the crystal structure two CN groups of [B(CN)₄][−] are coordinated by Mg²⁺ and they correspond to the highest CN stretching frequencies. The two other CN groups are coordinated by H₂O and correlate with the band at 2246 cm^{−1}. The lowest CN stretch at 2234 cm^{−1} is typical for non coordinated CN as in [Mg(H₂O)₆][B(CN)₄]₂ (observed at about 2237 cm^{−1} in the Raman spectrum). Presumably this band in Figure 11 is due to an [Mg(H₂O)₆][B(CN)₄]₂ impurity. In anhydrous Mg[B(CN)₄]₂ most likely three CN groups are strong coordinated by Mg²⁺ (2280 cm^{−1}) and one CN group is not coordinated at all (2234 cm^{−1}).

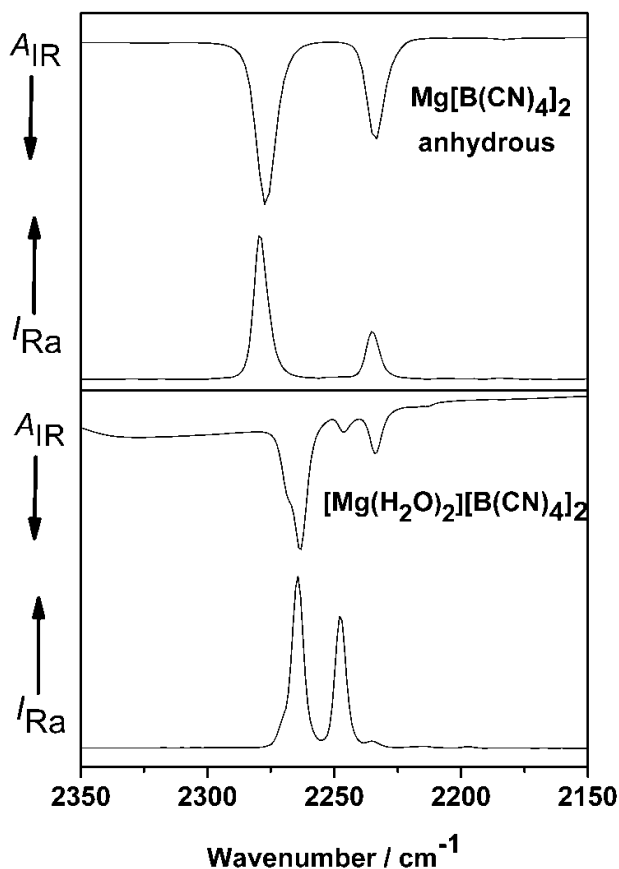


Fig. 11. IR spectrum (top) and Raman spectrum (bottom) of anhydrous Mg[B(CN)₄]₂ (upper part) and [Mg(H₂O)₂][B(CN)₄]₂ (lower part).

A consideration of the vibrational data of known [B(CN)₄][−] salts shows that the wave numbers of the CN stretching mode increases with decreasing radii of the metal cations, because the lone pair (σ -CN orbital) is lowered in energy by the *M*⋯N–C interaction, causing a strengthening of the C–N bond. Hence, the CN stretching frequency increases with the strength of the interionic contacts. This trend found within tetracyanidoborates

with singly charged cations could be validated with tetracyanidoborates with divalent cations as counter ions as well.

In all alkali metal tetracyanidoborate salts only one CN stretching mode in the region $2220\text{--}2270\text{ cm}^{-1}$ could be observed in the Raman spectra, because the A_1 and T_2 modes are accidentally degenerated. The reason can be seen in a lack of coupling between the CN stretching modes as no π -back-bonding between the boron atom and the CN ligands occurs. The first discovered exception of a tetracyanidoborate salt with a single charged cation is $\text{Cu}[\text{B}(\text{CN})_4]$.^{1,14a}

The calcium salt $[\text{Ca}(\text{H}_2\text{O})_3][\text{B}(\text{CN})_4]_2$ shows in the IR spectra two bands at 2244 and 2256 cm^{-1} . In comparison to the dehydrated salt $\text{Ca}[\text{B}(\text{CN})_4]_2$ (bands at 2233 and 2264 cm^{-1}) the CN stretching mode is shifted to a lower wave number. The spectra of both salts are shown in Figure 12. The reason for the different frequencies is the different coordination pattern of the central atom due to the competition of the water molecules and the nitrogen atom of the cyano groups. The Raman spectrum shows two additional bands at 2233 and 2264 cm^{-1} , presumably due to some anhydrous calcium salt.

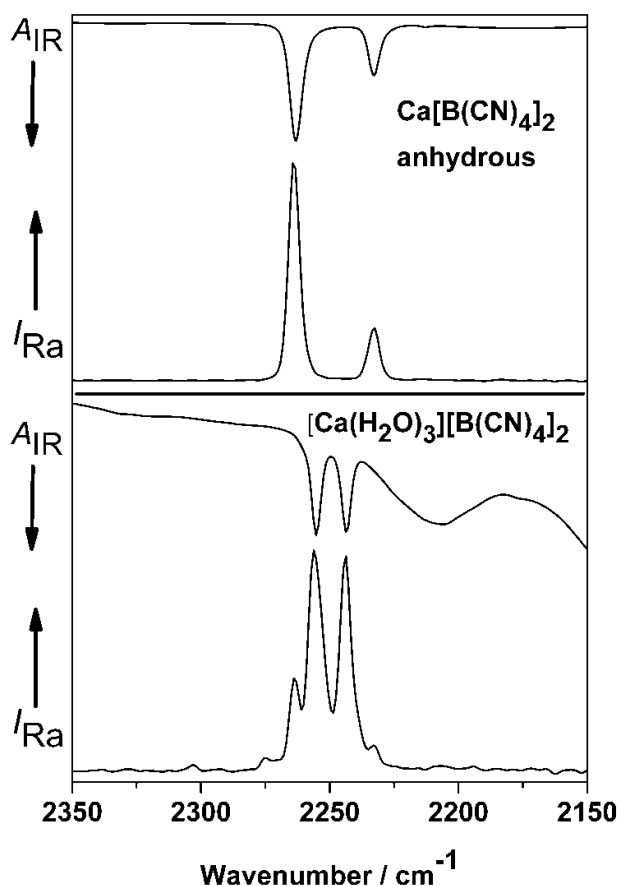


Fig. 12. IR spectrum (top) and Raman spectrum (bottom) of anhydrous $\text{Ca}[\text{B}(\text{CN})_4]_2$ (upper part) and $[\text{Ca}(\text{H}_2\text{O})_3][\text{B}(\text{CN})_4]_2$ (lower part). The sample for the Raman measurement contained besides $[\text{Ca}(\text{H}_2\text{O})_3][\text{B}(\text{CN})_4]_2$ also of small amounts of the anhydrous compound.

The stretching mode at 2233 cm^{-1} is the frequency of the non-coordinating CN group. The stretching mode of the very weak coordinating CN group in tetrabutylammonium tetracyanidoborate is located at 2222 cm^{-1} .¹ In the region of the CN stretching modes the bands in the IR spectra coincide with the bands in the Raman spectra in both cases, in $[\text{Ca}(\text{H}_2\text{O})_3][\text{B}(\text{CN})_4]_2$ and $\text{Ca}[\text{B}(\text{CN})_4]_2$, respectively.

Whereas in the IR spectrum of **2**, **4**, and **5** the CN stretching mode is weak, that of **3** is of medium intensity. Because of very weak ionic interactions between the $[\text{Mg}^{\text{II}}(\text{DMF})_6]^{2+}$ cation and the tetracyanidoborate anion the IR and Raman spectrum of $[\text{Mg}^{\text{II}}(\text{DMF})_6][\text{B}(\text{CN})_4]_2$ shows only one CN band at 2222 cm^{-1} . This value compares well with the wave number found, for example, in $[\text{Bu}_4\text{N}][\text{B}(\text{CN})_4]$ or $(\text{BMIm})[\text{B}(\text{CN})_4]$ (Bu: butyl, BMIm: 1-butyl-3-methyl-imidazolium).¹

The CO stretching mode of the DMF molecules can be assigned to the band at 1654 cm^{-1} in the IR and 1644 cm^{-1} in the Raman spectrum, which is lower than that in free DMF molecules (1687 cm^{-1})²⁴ due to the coordination of the DMF oxygen atoms to the magnesium(II) ion. The result is a weakened C–O bond and hence a lower wave number. In $[\text{Fe}(\text{DMF})_6][\text{B}(\text{CN})_4]_2$ and $[\text{Zn}(\text{DMF})_6][\text{B}(\text{CN})_4]_2$ the CO stretching modes are detected at 1641 and 1644 cm^{-1} in the IR spectrum. This trend correlates with the Lewis acid strength respectively the radii of the metal ions. The other modes of the coordinated DMF molecule are nearly similar to those of the free solvent molecules. Those which are affected by the coordination to the magnesium(II) ion can be found at slightly lower wave numbers than in the non-coordinated DMF molecules.

Thermal properties

The DSC curve of the magnesium salt $[\text{Mg}(\text{H}_2\text{O})_2][\text{B}(\text{CN})_4]_2$ shows two peaks. The water molecules are removed at $155\text{ }^\circ\text{C}$ with an endothermic energy of 78 kJ mol^{-1} . The salt decomposes without melting at $582\text{ }^\circ\text{C}$ (114 kJ mol^{-1}).

After drying in high vacuum ($4.7 \cdot 10^{-7}$ mbar) at ca. $170\text{ }^\circ\text{C}$ over a period of 8 h the salt was measured again. This curve does not show any endothermic peak due to the complete dehydration. The decomposition temperature is with $586\text{ }^\circ\text{C}$ nearly identical to the temperature measured for the hydrated salt. Table 5 compares the dehydration and decomposition temperatures as well as the dehydration enthalpies of the title compounds **2** and **4** with those of $[\text{M}^{\text{II}}(\text{H}_2\text{O})_2][\text{B}(\text{CN})_4]_2$ ($\text{M}^{\text{II}} = \text{Co}, \text{Zn}, \text{Fe}$).

Tab. 5. Dehydration, decomposition and dehydration temperatures (onset temperatures) and dehydration enthalpies of $[\text{M}^{\text{II}}(\text{H}_2\text{O})_2][\text{B}(\text{CN})_4]_2$ ($\text{M}^{\text{II}} = \text{Co}, \text{Zn}, \text{Fe}$, and Mg) and $[\text{Ca}(\text{H}_2\text{O})_3][\text{B}(\text{CN})_4]_2$.

compound	dehydration temp./ $^\circ\text{C}$	dehydration enthalpie/ $\text{kJ}\cdot\text{mol}^{-1}$	decomposition temp./ $^\circ\text{C}$
$[\text{Co}(\text{H}_2\text{O})_2][\text{B}(\text{CN})_4]_2$	108-130	89.2	510
$[\text{Zn}(\text{H}_2\text{O})_2][\text{B}(\text{CN})_4]_2$	110-130	100.4	473
$[\text{Fe}(\text{H}_2\text{O})_2][\text{B}(\text{CN})_4]_2$	133-155	116.4	550
$[\text{Mg}(\text{H}_2\text{O})_2][\text{B}(\text{CN})_4]_2$	148-182	103.9	582
$[\text{Ca}(\text{H}_2\text{O})_3][\text{B}(\text{CN})_4]_2$	128-130	116	563

The calcium tetracyanidoborate $[\text{Ca}(\text{H}_2\text{O})_3][\text{B}(\text{CN})_4]_2$ shows an endothermic peak at 128 °C (116 kJ mol⁻¹), which is about 20 °C lower than in the magnesium salt. This is the result of the different chemical bonding of the water molecules. The substance decomposes at 563 °C. After drying (1x10⁻⁶ mbar / 85 °C / 16 h) this temperature is shifted to a value of 555 °C; no additional peak could be observed.

The trend of increasing decomposition temperatures with increasing lattice energies has been found also within the group 12 element tetracyanidoborates (Zn, Cd, Hg).^{2,14a,15} The smaller the cation the higher is the decomposition temperature. The melting points of the alkaline metal tetracyanidoborates follow the same trend.¹

As a first approximation, the melting points correlate with the estimated lattice energies, as shown within the alkaline metal tetracyanidoborates.¹ Due to the lower lattice energies of the tetracyanidoborates with singly charged cations, these salts melt before thermal decomposition.

In contrast to $[\text{Fe}(\text{DMF})_6][\text{B}(\text{CN})_4]_2$ ¹⁷ compound **3** does not lose any molecules of coordinated DMF ligands at room temperature. The DSC curve of $[\text{Mg}(\text{DMF})_6][\text{B}(\text{CN})_4]_2$ shows in the temperature range from 25 to 600 °C a sharp endothermic peak at 90 °C (onset). By heating the compound with the aid of a Boetius apparatus, the melting point has been detected at slightly higher temperature. Thus, the endothermic effect at 90 °C in the DSC corresponds to the melting point. The DSC curve shows a second endothermic peak at 250 °C (onset). At this temperature crystal formation has been observed. It is likely that the coordinated DMF molecules vaporize at 250 °C and leave the solvent-free compound $\text{Mg}[\text{B}(\text{CN})_4]_2$, which crystallizes. Exothermic decomposition takes place at the same temperature as that found for $[\text{Mg}(\text{H}_2\text{O})_2][\text{B}(\text{CN})_4]_2$, respectively $\text{Mg}[\text{B}(\text{CN})_4]_2$.

Conclusions

This paper describes the first salts with weakly coordinating tetracyanidoborate anions and alkaline metal cations. Five new compounds with Mg^{2+} or Ca^{2+} ions are presented. Depending on the type of cation different synthetic procedures were used to get the new compounds in high yields. Results from X-ray structure determinations show that $[\text{Mg}(\text{H}_2\text{O})_6][\text{B}(\text{CN})_4]_2$ and $[\text{Mg}(\text{DMF})_6][\text{B}(\text{CN})_4]_2$ are build up from isolated ions, whereas the other three compounds comprise different coordination polymers. All compounds lose the coordinated solvent molecules at elevated temperatures. They decompose above 500 °C before melting. Also, spectral features are reported.

Experimental Section

General Remarks

All starting materials were used as received. $\text{K}[\text{B}(\text{CN})_4]$ was synthesized by a high temperature method according to ref. 12. Starting from the potassium salt an aqueous solution of $\text{H}[\text{B}(\text{CN})_4]$ is obtained through an ion exchange process.²⁰ The sodium salt $\text{Na}[\text{B}(\text{CN})_4]$ is also synthesized according to ref. 12.

Safety Notes! Cyanides are highly toxic, especially if dissolved in organic solvents. On contact with acidic materials they can evolve

highly toxic HCN gas. They must always be handled with sufficient precaution.

Vibrational spectra: Infrared spectra in the range from 4000 - 500 cm⁻¹ were recorded with an evacuable FTIR-Spektrometer IFS 66v (Bruker Optics GmbH, Ettlingen, Germany) The spectral resolution is 2 cm⁻¹ utilizing a DTGS detector and a Ge/KBr beamsplitter. For each spectrum a total of 64 scans were recorded. The powdered samples were immersed in Nujol, which was sandwiched between AgBr disks.

The IR spectrum of $[\text{Mg}^{\text{II}}(\text{DMF})_6][\text{B}(\text{CN})_4]_2$ in the range of 4000-500 cm⁻¹ was obtained with a Nicolet 380 FT-IR spectrometer with a Smart Endurance ATR device. The according Raman spectrum was recorded at room temperature with a Bruker Vertex 70 Raman spectrometer (Bruker, Karlsruhe, Germany) by using the 1064 nm exciting line of a Nd/YAG laser.

Raman data (3500 - 50 cm⁻¹) of the title compounds **2**, **4**, and **5** were recorded at room temperature with a FT-Raman-Spektrometer Equinox 55 (Bruker Optics GmbH, Ettlingen, Germany) using the 1064 nm line (500 mW) of a Nd-YAG laser. The samples were sealed in glass capillaries of 2 mm outer diameter. The spectra were obtained by adding 512 scans, which were recorded with a resolution of 2 cm⁻¹.

Synthesis of $[\text{Mg}(\text{H}_2\text{O})_6][\text{B}(\text{CN})_4]_2$ (1) and $[\text{Mg}(\text{H}_2\text{O})_2][\text{B}(\text{CN})_4]_2$ (2): An amount of 0.238 g (9.79 mmol) of elemental magnesium (Merck Schuchardt, Hohenbrunn, Germany, 0,06 - 0,3 mm, purity > 98 %) is treated with 50 ml of a 0.1 M solution of $\text{H}[\text{B}(\text{CN})_4]$. A vigorous evolution of H₂ gas starts immediately. With stirring of the suspension at room temperature it lasts about 30 minutes. Stirring is continued for 16 hours. Then, the suspension is filtered and the solvent of the clear solution is removed completely in vacuum at room temperature. Yield: quantitative with respect to the acid. Analysis calculated for $\text{C}_8\text{H}_4\text{B}_2\text{MgN}_8\text{O}_2$ (**2**) ($M_r = 290,10$ g·mol⁻¹): C 33.12 %; H 1.39 %; N 38.63 %; Found: C 33.42 %, H 0.70 %; N 37.83 %.

An anhydrous material can be obtained in vacuum (5·10⁻⁷ mbar) by heating at 170 °C for at least 12 hr.

Crystals of **1** are obtained through evaporation of the water solvent from solutions of **2** at temperatures lower than 20 °C, those of **2** at temperatures higher than 20 °C.

Synthesis of $[\text{Mg}(\text{DMF})_6][\text{B}(\text{CN})_4]_2$ (3): $[\text{Mg}(\text{DMF})_6][\text{B}(\text{CN})_4]_2$ was synthesized by dissolving anhydrous $\text{Mg}[\text{B}(\text{CN})_4]_2$ in dry dimethylformamide. For this reaction 107 mg of $[\text{Mg}(\text{H}_2\text{O})_2][\text{B}(\text{CN})_4]_2$, which was synthesized as described above, was dried at 170 °C in an open glass tube in a tube furnace. After drying 93,6 mg (0.37 mmol) of the anhydrous material was obtained and dissolved in 0.5 mL (0.47 g, 6.43 mmol) of dry DMF in a 25 mL round-bottomed flask. The solvent was slowly evaporated at room temperature in a drybox, and colorless single crystals were obtained, which were suitable for a single-crystal X-ray structure determination. The yield of $[\text{Mg}(\text{DMF})_6][\text{B}(\text{CN})_4]_2$ was 0.247 g (97%). Anal. Calcd for $\text{C}_{26}\text{B}_2\text{N}_{14}\text{H}_{42}\text{O}_6\text{Mg}$ ($M_r = 692.64$ g·mol⁻¹): C, 45,09; N, 28,31; H, 6,11. Found: C, 43,891; N, 28,12; H, 5,81. IR (ATR, cm⁻¹ v_{max}): 2938, 2818, 2222, 1654, 1499, 1441, 1421, 1383, 1255, 1112, 1063, 989, 967, 929, 872, 866, 841, 820, 687. Raman (cm⁻¹ v_{max}): 2942, 2818, 2222, 1644, 1441, 1422, 1381, 1115, 868, 693, 679, 519, 485, 413, 388, 377, 143, 114, 68.

¹H-NMR (CDCl₃, 300 MHz): δ = 2,95 ppm (t, 3H, -CH₃); 3,08 ppm (t, 3H, -CH₃); 7,9 ppm (s, 1H, HCO); ¹³C-NMR (CDCl₃, 75 MHz): δ = 32,2 ppm (CH₃); 37,5 ppm (CH₃); 120,7 ppm (CN); 121,6 ppm (CN); 122,6 ppm (CN); 123,5 ppm (CN); 163,7 ppm (HCO) ¹¹B-NMR (CDCl₃, 96 MHz): δ = -38,2 ppm.

Synthesis of [Ca(H₂O)₃][B(CN)₄]₂ (4): A total of 13.798 g (100 mmol) Na[B(CN)₄] is dissolved in 100 mL H₂O and acidified with 18.5 mL (~200 mmol) of HCl_(conc.). Under vigorous stirring 38.5 mL (203 mmol) tri-*n*-propylamin (Merck-Schuchardt, Hohenbrunn, Germany, purity >98 %) are added. (⁹Pr₃NH)[B(CN)₄] is extracted from this solution using 250 mL, 100 mL, and finally 50 mL CH₂Cl₂. The combined organic solution is treated with 15.37 g (207 mmol) Ca(OH)₂ (Janssen Chimica, Geel, Belgium, 98+ %) and ~5 ml H₂O. After about 30 min of stirring a white precipitate solidifies and is filtered off the methylenechloride solution. The solid is extracted three times with THF (250 mL, 150 mL, and 50 mL) and the combined solution dried with calcium carbonate (E. Merck, Darmstadt, Germany, min. 99.5 %). After filtering the solvents is removed and the resulting white solid is washed with CH₂Cl₂. Yield: 3.986 g, 29.5 %. Analysis calculated for C₈H₄B₂CaN₈O₂ (Mr = 305.87 g·mol⁻¹): C 31.41 %; H 1.32 %; N 36.63 %; Found: C 32.66 %, H 1.10 %; N 37.40 %.

This compound can be dehydrated by heating at 85 °C for at least 16 hrs. at a pressure of about 1·10⁻⁶ mbar.

Synthesis of [Ca(H₂O)₂(CH₃CN)][B(CN)₄]₂ (5): Samples of the hydrate [Ca(H₂O)₃][B(CN)₄]₂ are dissolved in acetonitrile. Slow evaporation of the solvent gives **5** in quantitative yield.

DSC Measurements: Thermo-analytical measurements were performed using a Netzsch DSC 204 instrument (Netzsch GmbH, Selb, Germany). About 5 - 10 mg of the solid samples were weighed and sealed in aluminum crucibles. The used temperature range was from 20 to 600 °C with a heating rate of 10 K min⁻¹. Throughout the measurements the furnace was flushed with dry nitrogen.

The differential scanning calorimetry (DSC) measurement on [Mg^{II}(DMF)₆][B(CN)₄]₂ was carried out with a DSC 823e Mettler Toledo apparatus. The sample was heated up to 600 °C.

Elemental Analysis: The elemental analyses were accomplished by the microanalytical combustion methods at the Euro EA3000 (HEKA-Tech GmbH, Wegberg, Germany). The error margins for the determination of the elements were: C ±0,3 %, H ±0,51 % and N ±0,2 %.

X-ray Crystallography: Data for the X-ray structure determinations were collected on the following diffractometer systems:

a) For **1** on an Oxford Diffraction Gemini E Ultra diffractometer, equipped with a 2K×2K EOS CCD area detector, a four-circle κ goniometer, an Oxford Instruments Cryojet, and sealed-tube Enhanced (Mo) and the Enhanced Ultra (Cu) sources. For data collection, the Cu source emitting monochromated Cu Kα radiation (λ = 1.54184 Å) or Mo Kα radiation (λ = 0.71073 Å) was used. The diffractometer was controlled by the CrysAlisPro Graphical User Interface (GUI) software.²⁶ Processing of the raw data, scaling of diffraction data, and the application of an empirical absorption correction was completed by using the CrysAlisPro program.²⁶

b) For **2 – 5** on a Bruker-Nonius APEX-X8 diffractometer equipped with a CCD detector. Graphite monochromated MoKα radiation (λ = 0.71073 Å) was used. Single crystals were glued with canadian balsam on top of a glass fiber and mounted on the goniometer. First unit cell dimensions were determined from the reflections of 60 frames measured in 3 different crystal directions. Data collection was done using the Bruker-Nonius APEX-2, vers. 1.6-8 software,²⁷ and the data reduction including corrections for background, Lorenz and polarization effects using the SAINT program, vers. 7.06A.²⁷ Empirical absorption corrections based on comparison of redundant and equivalent reflections were applied (SADABS²⁷).

The structures were solved via direct methods. The structural models were completed using difference Fourier maps and refined by full-matrix least-squares methods on F². All atoms except hydrogen were refined using anisotropic thermal parameters. Hydrogen atoms were refined isotropically (**1**) or fixed on idealized positions and refined with isotropic thermal parameters based on the bonded atom (**2 – 5**). All calculations were performed on PCs using the SHELX-97 programs²⁸ or the WinGX program system.²⁹ Structural graphics were produced with the aid of the Diamond program.³⁰ Crystal data, data collection, and refinement parameters for are given in Table 1. Further details of the crystal-structure investigations are supplied in CIF format. This material is available free of charge via the CCDC data centre,

CCDC-893429 for **1**, CCDC-705243 for **2**, CCDC-884526 for **3**, CCDC-705245 for **4**, and CCDC-705244 for **5**, free of charge via <http://www.ccdc.cam.ac.uk>, or from the Cambridge Crystallographic Data Centre, 12 Union Road, Cambridge CB21EZ, UK; Fax: (+44) 1223-336-033; or E-mail: deposit@ccdc.cam.ac.uk

For **2**, another CCDC dataset exists for a measurement at 150 K; CCDC-893430.

Acknowledgments

Financial support from the Deutsche Forschungsgemeinschaft of Germany is gratefully acknowledged. We also thank Prof. Reinke and Dr. Villinger (Rostock) for providing X-ray equipment.

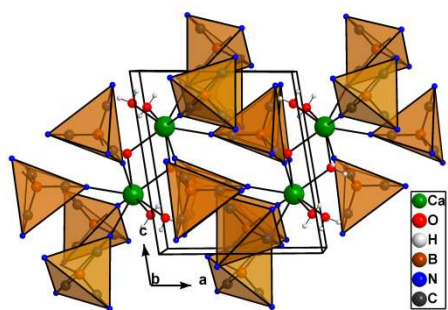
Notes and references

- 1 T. Küppers, E. Bernhardt, H. Willner, H. W. Rohm, M. Köckerling, *Inorg. Chem.* **2005**, *44*, 1015-1022.
- 2 M. Berkei, E. Bernhardt, M. Schürmann, M. Mehring, H. Willner, *Z. Anorg. Allg. Chem.* **2002**, *628*, 1734-1740.
- 3 B. H. Hamilton, C. J. Ziegler, *J. Chem. Soc., Chem. Commun.* **2002**, 842-843.
- 4 M. L. Kuhlmann, H. Yao, T. B. Rauchfuss, *J. Chem. Soc., Chem. Commun.* **2004**, 1370-1371.
- 5 D. Williams, B. Pleune, B.; Kouvetakis, J.; 537 Williams, M. D.; Andersen, R. A. *J. Am. Chem. Soc.* **2000**, *122*, 7735-7741.
- 6 (a) E. Bernhardt, M. Finze, H. Willner, C. W. Lehmann, F. Aubke, *Angew. Chem.* **2003**, *115*, 2123-2125; (b) W. W. Wilson, A. Vij, V. Vij, E. Bernhardt, K. O. Christe, *Chem. Eur. J.* **2003**, *9*, 2840-2844.
- 7 (a) M. L. Kuhlmann, H. Yao, T. B. Rauchfuss, *Chem. Commun.* **2004**, 1370-1371; (b) E. Bernhardt, M. Berkei, H. Willner, M. Schürmann, *Z. Anorg. Allg. Chem.* **2003**, *629*, 677-685; (c) E. Bernhardt, G. Henkel, H. Willner, G. Pawelke, H. Bürger, *Chem. Eur. J.* **2001**, *7*, 4696-4705; (d) U. Welz-Biermann, N. V. Ignatiev, E. Bernhardt, M. Finze, H. Willner, *WO-072089*, **2004**; (e) B. H. Hamilton, C. J. Ziegler, *Chem. Commun.* **2002**, 842-843; (f) M. Finze, E. Bernhardt, A. Terheiden, M. Berkei, H. Willner, D. Christen, H. Oberhammer, F. Aubke, *J. Am. Chem. Soc.* **2002**, *124*,

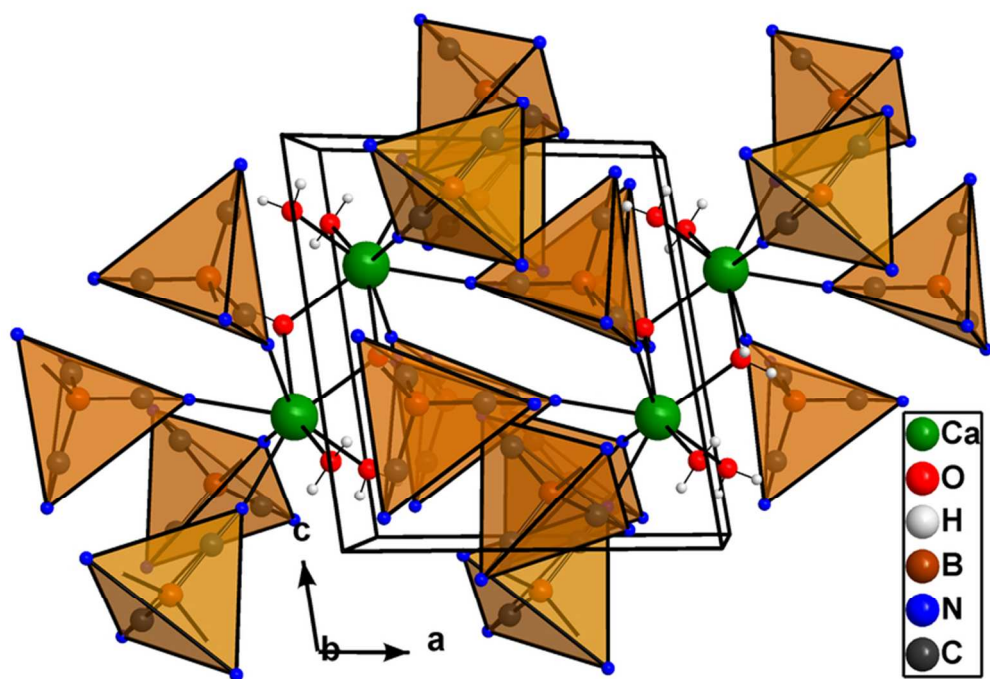
- 15385–15398; (g) A. Terheiden, E. Bernhardt, H. Willner, F. Aubke, *Angew. Chem.* **2002**, *114*, 823–825.
- 8 (a) A. Bernsdorf, H. Brand, R. Hellmann, M. Köckerling, A. Schulz, A. Villinger, C. Voss, *J. Am. Chem. Soc.* **2009**, *131*, 8958–8970; (b) M. Finze, PhD-thesis, University of Hannover (Germany), **2004**.
- 9 see for example: (a) I. Krossing, I. Raabe, *Angew. Chem. Int. Ed.* **2004**, *43*, 2066 – 2090; *Angew. Chem.* **2004**, *116*, 2116–2142 (b) S. H. Strauss, *Chem. Rev.* **1993**, *93*, 927–942; (c) W. Beck, K. Sünkel, *Chem. Rev.* **1988**, *88*, 1405–1421.
- 10 (a) U. Welz-Biermann, N. V. Ignatiev, E. Bernhardt, M. Finze, H. Willner, Merck Patent GmbH, Darmstadt, *WO 2004/072089 A1*, **2004**; (b) N. V. Ignatiev, U. Welz-Biermann, A. Kuchcrynina, G. Bissky, H. Willner, *J. Fluorine Chem.* **2005**, *126*, 1150–1159; (c) D. Kuang, P. Wang, S. Ito, S. M. Zakeeruddin, M. Grätzel, *J. Am. Chem. Soc.* **2006**, *128*, 7732–7733; (d) Y. Bai, Y. Cao, J. Zhang, M. Wang, R. Li, P. Wang, S. M. Zakeeruddin, M. Grätzel, *Nat. Mater.* **2008**, *7*, 626–630 and references cited therein; (e) D. Shi, Y. Cao, N. Pootrakulchote, Z. Yi, M. Xu, S. M. Zakeeruddin, M. Grätzel, P. Wang, *J. Phys. Chem. C* **2008**, *112*, 17478–17485; (f) D. Shi, N. Pootrakulchote, R. Li, J. Guo, Y. Wang, S. M. Zakeeruddin, M. Grätzel, P. Wang, *J. Phys. Chem. C* **2008**, *112*, 17046–17050; (g) M. Xu, S. Wenger, H. Bala, D. Shi, R. Li, Y. Zhou, S. M. Zakeeruddin, M. Grätzel, P. Wang, *J. Phys. Chem. C* **2009**, *113*, 2966–2973.
- 11 (a) P. Izák, M. Köckerling, U. Kragl, *Green Chem.* **2006**, *8*, 947–948; (b) P. Izák, M. Köckerling, U. Kragl, *Desalination* **2006**, *199*, 96–98; (c) P. Izák, K. Friess, V. Hynek, W. Ruth, Z. Fei, J. P. Dyson, U. Kragl, *Desalination* **2009**, *241*, 182–187; (d) P. Izák, W. Ruth, Z. Fei, J. P. Dyson, U. Kragl, *Chem. Eng. J.* **2008**, *139*, 318–321.
- 12 E. Bernhardt, M. Finze, H. Willner, *Z. Anorg. Allg. Chem.* **2003**, *629*, 1229–1234.
- 13 E. Bernhardt, G. Henkel, H. Willner, *Z. Anorg. Allg. Chem.* **2000**, *626*, 560–568.
- 14 (a) M. Neukirch, S. Tragl, H. J. Meyer, T. Küppers, H. Willner, *Z. Anorg. Allg. Chem.* **2006**, *632*, 939–944; (b) M. Finze, E. Bernhardt, M. Berkei, H. Willner, J. Hung, R. M. Waymouth, *Organometallics* **2005**, *24*, 2103–5109.
- 15 M. Neukirch, Dissertation, University of Tübingen, **2007**.
- 16 C. Nitschke, M. Köckerling, *Z. Anorg. Allg. Chem.* **2009**, *635*, 503–507.
- 17 C. Nitschke, M. Köckerling, *Inorg. Chem.*, **2011**, *50*, 4313–4321.
- 18 A. Flemming, M. Hoffmann, M. Köckerling, *Z. Anorg. Allg. Chem.* **2010**, *636*, 562–568.
- 19 A. Bernsdorf, M. Köckerling, *Eur. J. Inorg. Chem.* **2009** 4547–4553.
- 20 T. Küppers, E. Bernhardt, C. W. Lehmann, H. Willner, *Z. Anorg. Allg. Chem.* **2007**, *633*, 1666–1672.
- 21 R. D. Shannon, *Acta Cryst. A* **1976**, *32*, 751–767.
- 22 See, for example: (a) B. Weber, E. Kaps, J. Weiga, K. Achterhold, F. G. Parak, *Inorg. Chem.* **2008**, *47*, 487–496; (b) D. W. Blakesley, S. C. Payne, K. S. Hagen, *Inorg. Chem.* **2000**, *39*, 1979–1989.
- 23 C. Nitschke, M. Köckerling, so far unpublished research.
- 24 B. L. Barker, D. Aubry, F. R. Fronczek, S. F. Watkins, G. G. Stanley, *Acta Cryst. E* **2006**, *62*, m942–m944.
- 25 T. S. Piper, E. G. Rochow, *J. Am. Chem. Soc.* **1954**, *76*, 4318–4320.
- 26 CrysAlisPro, version 1.171.33.42; Oxford Diffraction Ltd: Oxford, U. K.
- 27 Apex-2, v. 1.6-8, Saint, v. 6.25, SADABS-Software for the CCD detector System; Bruker-Nonius Inc., Madison, WI, **2003**.
- 28 (a) G. M. Sheldrick, SHELX97-Programs for crystal structure analysis (Release 97-2); University of Göttingen: Göttingen, Germany, 1997. (b) G. M. Sheldrick, *Acta Crystallogr. A.*, **2008**, *64*, 112–122.
- 29 L. J. Farrugia, WinGX v1.64.05 (**2003**) – An Integrated System of Windows Programs for the Solution, Refinement and Analysis of Single Crystal X-ray Diffraction Data; University Glasgow: Glasgow, Scotland, *J. Appl. Crystallogr.* **1999**, *32*, 837–838.
- 30 K. Brandenburg, Diamond, version.3.2i; Crystal Impact GbR: Bonn, Germany, 2012.

Received: ((will be filled in by the editorial staff))
Published online: ((will be filled in by the editorial staff))

TOC-Entry



The syntheses, structures, spectra and thermal properties of the first tetracyanidoborate salts coordinating weakly to solvated alkaline earth cations are discussed.



70x49mm (300 x 300 DPI)